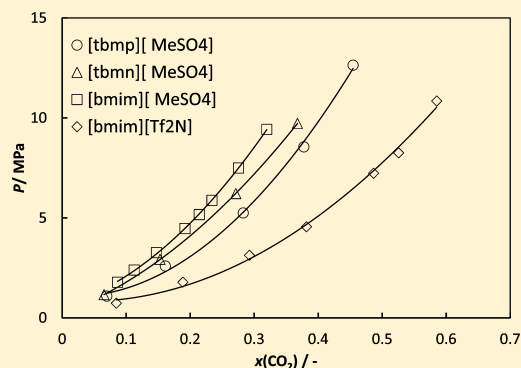


# Solubility of CO<sub>2</sub> in the Ionic Liquids [TBMN][MeSO<sub>4</sub>] and [TBMP][MeSO<sub>4</sub>]

Mahinder Ramdin, Thijs J. H. Vlucht, and Theo W. de Loos\*

Engineering Thermodynamics, Process & Energy Department, Faculty of Mechanical, Maritime, and Materials Engineering, Delft University of Technology, Leeghwaterstraat 44, 2628 CA Delft, The Netherlands

**ABSTRACT:** The solubility of CO<sub>2</sub> in two inexpensive ionic liquids, tributylmethylammonium methylsulfate [TBMN][MeSO<sub>4</sub>] and tributylmethylphosphonium methylsulfate [TBMP][MeSO<sub>4</sub>], has been studied experimentally. A synthetic method was used to measure bubble-point pressures up to 13 MPa for a temperature range of (313 to 368) K. The solubility of CO<sub>2</sub> in [TBMP][MeSO<sub>4</sub>] was slightly higher than in [TBMN][MeSO<sub>4</sub>], but CO<sub>2</sub> solubilities in both the ionic liquids were surprisingly higher than in the imidazolium analogue 1-butyl-3-methylimidazolium methylsulfate [bmim][MeSO<sub>4</sub>]. The relatively high melting points of the used ionic liquids may limit their application in CO<sub>2</sub> capture processes.



## INTRODUCTION

A decade has been passed since the breakthrough publication of Blanchard et al.<sup>1</sup> in *Nature*, showing the potential of ionic liquids (ILs) as green solvents. In the meanwhile, ILs have gained interest in many research areas like analytical chemistry,<sup>2</sup> biochemistry,<sup>3</sup> catalysis,<sup>4</sup> electrochemistry,<sup>5</sup> separation technology,<sup>6</sup> and many others. ILs are defined as salts that consist exclusively of ions and have melting points lower than 100 °C.<sup>3</sup> A remarkable application interest of ILs is their potential use in gas separation technology, especially for CO<sub>2</sub> capture from fluegas streams and natural gas. The amine-process currently used for CO<sub>2</sub> capture is extremely expensive and suffers many drawbacks as amines are corrosive, degradation sensitive, and volatile.<sup>7</sup> Some of these problems can be circumvented by using ILs since many ILs have negligible volatility, high chemical/thermal stability, and tunable properties.<sup>8</sup> The tunability of the properties of ILs allows the design of application-specific ILs by modifying the nature of the cations and anions. The imidazolium class of ILs for CO<sub>2</sub> capture has been studied in great detail by both experiments and computer simulations.<sup>9–15</sup> However, other classes of ILs such as ammonium,<sup>16–18</sup> phosphonium,<sup>19,20</sup> pyridinium,<sup>10,21,22</sup> and pyrrolidinium<sup>23–25</sup> ILs are since recently being explored for CO<sub>2</sub> capture. However, the number of commercial IL processes is scarce despite the huge number of scientific publications every year recognizing the well-known benefits of ILs over traditional solvents. Many of the barriers for commercializing IL-processes were addressed during a workshop entitled “Barriers to ionic liquid commercialization” held in New York in 2003.<sup>26</sup> In a recent review, Joglekar et al.<sup>27</sup> reported the main issues and barriers that impede successful application of ILs at industrial scale. One of the barriers identified by Joglekar et al. is the extremely high price (ca. \$1000/kg) of commonly used ILs. Although economy of scale should apply, it is unlikely that

complex molecules like ILs will reach a prize level comparable to that of traditional solvents. Nonetheless, the prize of ILs can be lowered significantly by using less complex molecules like ammonium or phosphonium ILs instead of the more complex and often more expensive imidazolium, pyridinium, or pyrrolidinium ILs. For a good choice, however, not the prize, but the price/performance ratio of an IL should be considered in order to select one IL over another.

This motivated us to select relatively inexpensive ammonium and phosphonium based ILs for CO<sub>2</sub> solubility measurements and to compare the performance of these ILs against the commonly used imidazolium counterparts. Hence, we have measured the CO<sub>2</sub> solubility in the ILs tributylmethylammonium methylsulfate [TBMN][MeSO<sub>4</sub>] and tributylmethylphosphonium methylsulfate [TBMP][MeSO<sub>4</sub>] in a temperature range of (313 to 368) K and up to 13 MPa. Furthermore, Henry’s constants for CO<sub>2</sub> in the two ILs have been determined from the experimental data. Subsequently, a comparison is given of the CO<sub>2</sub> solubilities in the two measured ILs and the available literature data of the imidazolium analogue.

## EXPERIMENTAL SECTION

The ILs tributylmethylammonium methylsulfate [TBMA]-[MeSO<sub>4</sub>] (>95 mol % purity) and tributylmethylphosphonium methylsulfate [TBMP][MeSO<sub>4</sub>] (>95 mol % purity) were purchased from Sigma-Aldrich. Prior to the experiments, the ILs were dried under moderate vacuum at 80 °C for several days. After drying the ILs, the water content was determined by

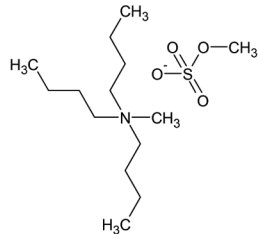
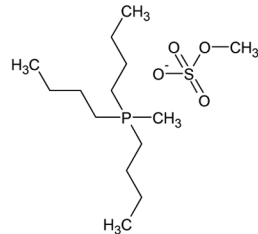
Received: February 27, 2012

Accepted: June 20, 2012

Published: July 6, 2012



Table 1. Properties of the Used ILs<sup>a</sup>

Structure		
Name	Tributylmethylammonium methylsulphate	Tributylmethylphosphonium methylsulphate
Abbreviation	[TBMA][MeSO <sub>4</sub> ]	[TBMP][MeSO <sub>4</sub> ]
Molar mass (g/mol)	311.48	328.45
Melting point (°C)	62	38
Purity (mole %)	> 95	> 95
Water content (ppm)	1800	850
Chloride content (mg/kg)	< 30	< 30

<sup>a</sup>The water content was measured with Karl Fischer titration, whereas the melting points and purities were reported by the supplier (Sigma-Aldrich).

Karl Fischer titration (Metrohm 756 KF Coulometer). Table 1 gives an overview of the IL properties, noting that the melting points were taken from the Material Safety Data Sheet (MSDS) of the supplier. We note that leaving the ILs for more than a week in the vacuum oven did not reduce the water content further, indicating the highly hygroscopic nature of these ILs. The sample preparation starts with filling a known amount of dried IL in a Pyrex glass tube. This tube with IL is then connected to a gas dosing system where the IL sample is degassed thoroughly under high vacuum by a repeatedly freezing and melting procedure. After degassing the sample, CO<sub>2</sub> is dosed using mercury through a calibrated vessel into the tube. The tube with a known composition is now disconnected from the dosing system and placed in the Cailletet apparatus, where the mercury serves as a pressurizing fluid. The experiments were performed in Cailletet equipment, which operates according to the synthetic method. The Cailletet equipment allows phase equilibria measurements within a pressure range of (0.1 to 15) MPa and a temperature range of (255 to 470) K. Here, only a brief description of the Cailletet apparatus is given because a detailed explanation can be found elsewhere.<sup>28–30</sup> A known composition of the CO<sub>2</sub>–IL mixture is enclosed in a Pyrex glass tube and placed in the Cailletet equipment. Subsequently, the temperature is fixed, and the pressure is gradually adjusted until the disappearance of the last gas-bubble, which corresponds to the bubble-point pressure, is observed visually. The solubility of CO<sub>2</sub> is determined by measuring the bubble-point pressures at different but fixed temperatures and compositions. The uncertainty in the temperature and pressure measurements of the Cailletet equipment is  $\pm 0.01$  K and  $\pm 0.005$  MPa, respectively. The uncertainty associated with the composition of the samples is  $\pm 0.001$  mol fraction. We have assumed that all volatile impurities have been removed during the high vacuum treatment of the sample and that the uncertainty in the mole fraction is calculated assuming that water is the only impurity present in an amount as given in Table 1. The carbon dioxide used in the experiments had a purity of 99.995 % and was supplied by The Linde Group.

## RESULTS AND DISCUSSION

Bubble-point pressures of CO<sub>2</sub> in the ILs [TBMA][MeSO<sub>4</sub>] and [TBMP][MeSO<sub>4</sub>] have been determined experimentally by a synthetic method. The results are given in Tables 2 and 3 for

**Table 2. Bubble Point Data of the System CO<sub>2</sub> (1) + [TBMA][MeSO<sub>4</sub>] (2), Where  $x_1$  Is the Mole Fraction of CO<sub>2</sub>,  $p$  the Bubble-Point Pressure,  $T$  the Temperature, and  $u(i)$  the Standard Uncertainties<sup>a</sup>**

$x_1$	$T/K$	$p/\text{MPa}$	$x_1$	$T/K$	$p/\text{MPa}$
0.066	338.35	1.009	0.153	338.40	2.450
0.066	343.29	1.059	0.153	343.40	2.610
0.066	348.40	1.109	0.153	348.36	2.760
0.066	353.39	1.164	0.153	353.45	2.930
0.066	358.48	1.214	0.153	358.48	3.080
0.066	363.48	1.284	0.153	363.49	3.196
0.066	368.41	1.334	0.153	368.41	3.401
0.271	338.41	5.138	0.368	338.40	8.029
0.271	343.44	5.493	0.368	343.29	8.574
0.271	348.48	5.837	0.368	348.40	9.174
0.271	353.53	6.228	0.368	353.35	9.741
0.271	358.56	6.558	0.368	358.43	10.337
0.271	363.50	6.914	0.368	363.41	10.953
0.271	368.63	7.319	0.368	368.45	11.528

<sup>a</sup> $u(x_1) = 0.001$ ;  $u(T) = 0.01$  K; and  $u(p) = 0.005$  MPa

the systems CO<sub>2</sub> + [TBMA][MeSO<sub>4</sub>] and CO<sub>2</sub> + [TBMP][MeSO<sub>4</sub>], respectively. These results are also shown graphically in Figures 1 and 2. With increasing temperature in both systems, the bubble-point pressure increases for a fixed composition.  $P$ – $x$  isothermal diagrams were constructed by interpolation from Figures 1 and 2. The  $P$ – $x$  diagrams, see Figures 3 and 4, show a trend typically observed for CO<sub>2</sub>–IL systems. CO<sub>2</sub> dissolves well in both ILs at low CO<sub>2</sub> mole fractions, but the bubble-point pressures increase sharply as the CO<sub>2</sub> mole fraction becomes higher. Figure 5 provides a comparison of the CO<sub>2</sub> solubilities in the two measured ILs and two imidazolium-based ILs from the literature.<sup>31,32</sup> CO<sub>2</sub> solubility in [TBMP][MeSO<sub>4</sub>] is slightly higher than in

**Table 3.** Bubble Point Data of the System CO<sub>2</sub> (1) + [TBMP][MeSO<sub>4</sub>] (2), Where  $x_1$  Is the Mole Fraction of CO<sub>2</sub>,  $p$  the Bubble-Point Pressure,  $T$  the Temperature, and  $u(i)$  the Standard Uncertainties<sup>a</sup>

$x_1$	$T/K$	$p/\text{MPa}$	$x_1$	$T/K$	$p/\text{MPa}$
0.070	313.20	0.659	0.161	313.16	1.504
0.070	323.20	0.759	0.161	323.14	1.770
0.070	333.24	0.873	0.161	333.12	2.040
0.070	343.20	0.979	0.161	343.11	2.365
0.070	353.26	1.089	0.161	353.11	2.595
0.070	363.25	1.209	0.161	363.13	2.900
0.283	313.16	3.089	0.378	313.22	5.011
0.283	323.10	3.554	0.378	323.15	5.836
0.283	333.12	4.130	0.378	333.14	6.657
0.283	343.14	4.675	0.378	343.19	7.577
0.283	353.18	5.250	0.378	353.18	8.553
0.283	363.13	5.815	0.378	363.30	9.659
0.455	313.20	6.746			
0.455	323.25	8.037			
0.455	333.22	9.447			
0.455	343.24	10.909			
0.455	353.27	12.640			

<sup>a</sup> $u(x_1) = 0.001$ ;  $u(T) = 0.01$  K; and  $u(p) = 0.005$  MPa

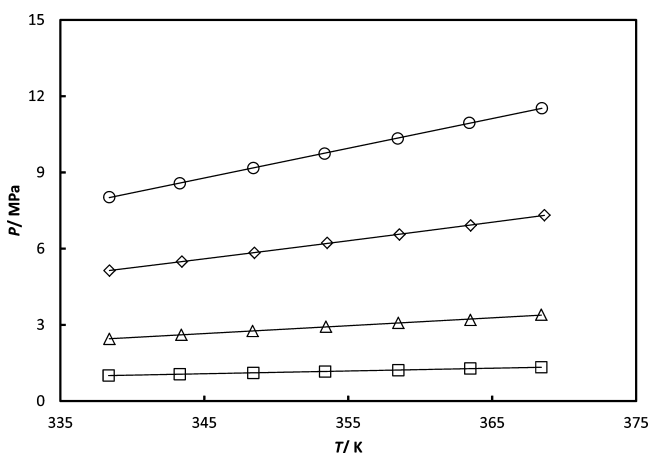


**Figure 1.** Isoleths of the system CO<sub>2</sub> + [tbma][MeSO<sub>4</sub>] for various carbon dioxide concentrations (mole %): squares, 6.6 %; triangles, 15.3 %; diamonds, 27.1 %; circles, 36.8 % . The lines through the data are polynomial fits to guide the eye.

[TBMA][MeSO<sub>4</sub>], but the CO<sub>2</sub> solubilities in both the ILs are surprisingly slightly higher than in the imidazolium analogue 1-butyl-3-methylimidazolium methylsulfate [bmim][MeSO<sub>4</sub>]. However, as it can be seen in Figure 5, the CO<sub>2</sub> solubility in ILs containing the [MeSO<sub>4</sub>] anion are significantly lower than in ILs containing a fluorinated anion (e.g., [bmim][Tf2N]). These results underpin the generally accepted finding that cations play a minor role in the dissolution of CO<sub>2</sub>, whereas the anions (especially the fluorinated ones) have a much larger effect on the CO<sub>2</sub> solubility.<sup>11</sup> Henry's law is often used to characterize gas solubilities in liquids. The Henry constant  $H_{12}$  of a solute 1 in a solvent 2 can be obtained from

$$H_{12} = \lim_{x_1 \rightarrow 0} \frac{f_1^L}{x_1} \quad (1)$$

where  $x_1$  is the CO<sub>2</sub> mole fraction and  $f_1^L$  the fugacity of the CO<sub>2</sub> in the liquid. Assuming that the vapor phase is pure CO<sub>2</sub>,  $f_1^L$

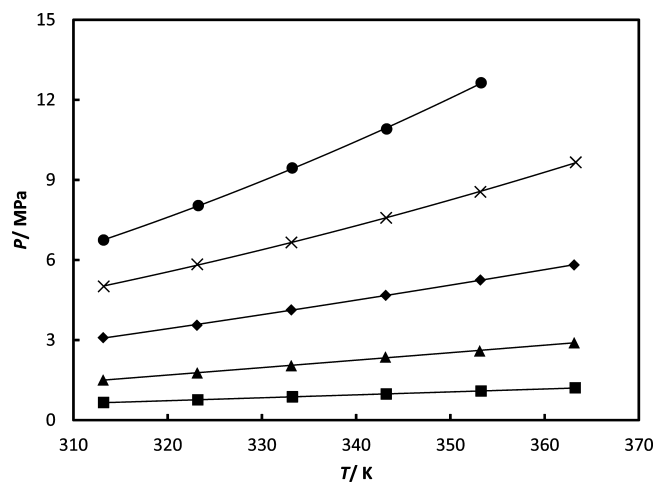


**Figure 2.** Isoleths of the system CO<sub>2</sub> + [tbmp][MeSO<sub>4</sub>] for various carbon dioxide concentrations (mole %): squares, 7.0 %; triangles, 16.1 %; diamonds, 28.3 %; crosses, 37.8 %; circles, 45.5 %. The lines through the data are polynomial fits to guide the eye.

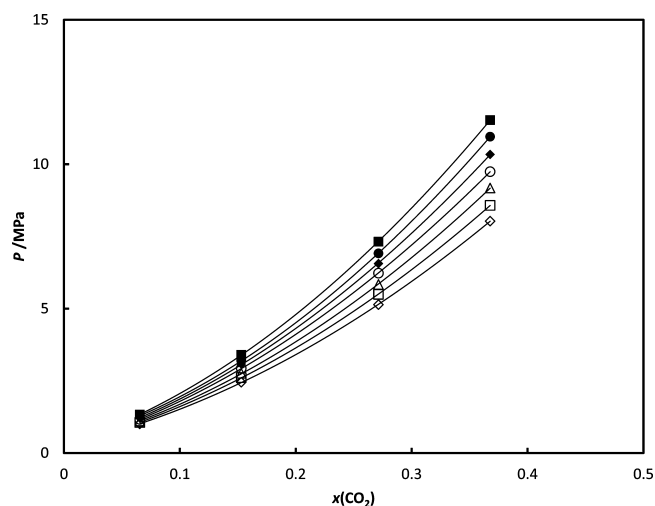


**Figure 3.**  $P$ - $x$  diagram of the system CO<sub>2</sub> + [tbma][MeSO<sub>4</sub>] at several temperatures: open diamonds, 338.15 K; open squares, 343.15 K; open triangles, 348.15 K; open circles, 353.15 K; filled diamonds, 358.15 K; filled circles, 363.15 K. The lines through the data are polynomial fits to guide the eye.

can be calculated at the experimental bubble-point pressure from the equation of state<sup>33</sup> of pure CO<sub>2</sub> from the equilibrium relationship

$$f_1^L = f_1^V \quad (2)$$

The Henry constants of CO<sub>2</sub> in the two ILs have been determined by plotting the fugacity of CO<sub>2</sub> as a function of the CO<sub>2</sub> mole fraction. An example of this is shown in Figure 6 for the system CO<sub>2</sub> + [TBMA][MeSO<sub>4</sub>], where the slope of the line is equivalent to the Henry constants. Similarly, the Henry constants for the system [TBMP][MeSO<sub>4</sub>] at different temperatures have been determined, and the results for both the systems are given in Table 4. A higher Henry constant corresponds to a lower CO<sub>2</sub> solubility in the IL; hence, the CO<sub>2</sub> solubility in [TBMP][MeSO<sub>4</sub>] is higher than in [TBMA][MeSO<sub>4</sub>] for the same temperature. The Henry constants of CO<sub>2</sub> in fluorinated ILs are generally much lower than the values reported here (e.g., the Henry constant of CO<sub>2</sub> in [bmim]-

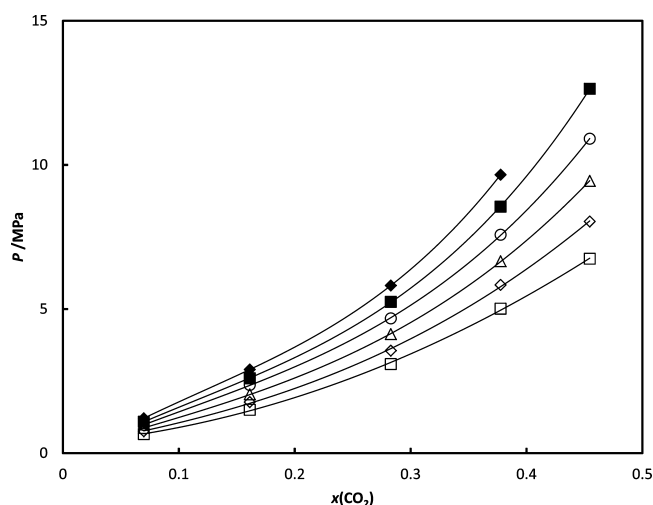


**Figure 4.**  $P$ - $x$  diagram of the system  $\text{CO}_2 + [\text{tbmp}][\text{MeSO}_4]$  at several temperatures: open squares, 313.15 K; open diamonds, 323.15 K; open triangles, 333.15 K; open circles, 343.15 K; filled squares, 353.15 K; filled diamonds, 363.15 K. The lines through the data are polynomial fits to guide the eye.

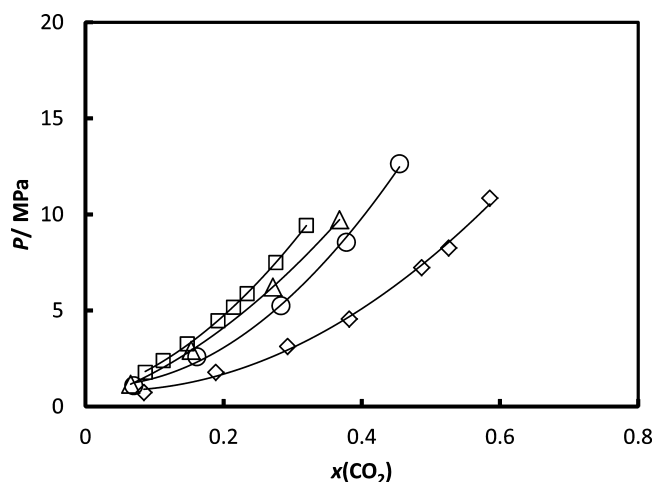


**Figure 5.** Isotherm at 353 K for the systems  $\text{CO}_2 + [\text{tbma}][\text{MeSO}_4]$  (triangles),  $[\text{tbmp}][\text{MeSO}_4]$  (circles),  $[\text{bmim}][\text{MeSO}_4]$  (squares), and  $[\text{bmim}][\text{Tf}_2\text{N}]$  (diamonds). Data of  $[\text{bmim}][\text{MeSO}_4]$  taken from Kumelan et al.<sup>31</sup> and  $[\text{bmim}][\text{Tf}_2\text{N}]$  data taken from Raeissi and Peters.<sup>32</sup> The lines through the data are polynomial fits to guide the eye.

$[\text{Tf}_2\text{N}]$  at 60 °C is around 4.8 MPa).<sup>10</sup> Furthermore, the enthalpy of absorption of  $\text{CO}_2$  in the two ILs has been determined using the following thermodynamic relationship:

$$\Delta_{\text{abs}} h^\infty = R \left( \frac{\partial \ln H_{12}}{\partial 1/T} \right)_p \quad (3)$$

Hence, the enthalpy of absorption can be determined by plotting the logarithm of the Henry constant against the reciprocal of the temperature, which is a straight line as shown in Figure 7. In this way, the enthalpy of absorption of  $\text{CO}_2$  in  $[\text{TBMA}][\text{MeSO}_4]$  and  $[\text{TBMP}][\text{MeSO}_4]$  has been determined to be  $-10.8$  kJ/mol and  $-12.1$  kJ/mol, respectively. The larger enthalpy of absorption of  $\text{CO}_2$  in  $[\text{TBMP}][\text{MeSO}_4]$  is consistent with the higher  $\text{CO}_2$  solubility observed in this IL. However,  $\text{CO}_2$  solubilities in the two investigated ILs are too low to be considered for  $\text{CO}_2$  capture at postcombustion

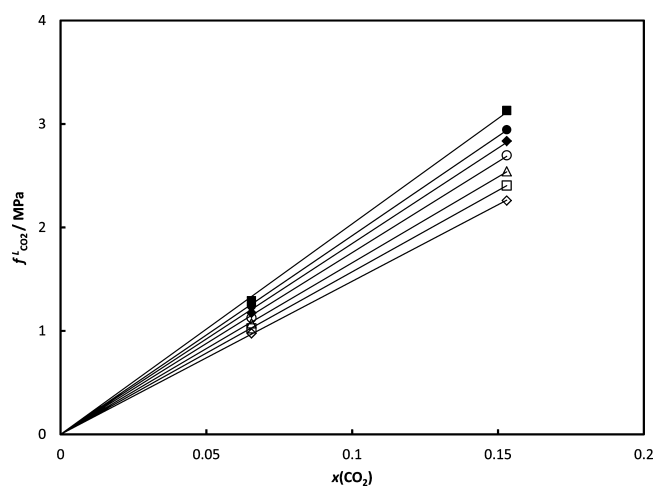


**Figure 6.** Fugacity of  $\text{CO}_2$  in the liquid ( $f_{\text{CO}_2}^L$ ) plotted against the  $\text{CO}_2$  mole fraction for the system  $\text{CO}_2 + [\text{tbma}][\text{MeSO}_4]$  to determine the Henry constant at several temperatures: open diamonds, 338.15 K; open squares, 343.15 K; open triangles, 348.15 K; open circles, 353.15 K; filled diamonds, 358.15 K; filled circles, 363.15 K; filled squares, 368.15 K.

**Table 4.** Henry Constants for  $\text{CO}_2$  in the Two Measured ILs at Several Temperatures

$\text{CO}_2 + [\text{TBMA}][\text{MeSO}_4]$		$\text{CO}_2 + [\text{TBMP}][\text{MeSO}_4]$	
$T/\text{K}$	$H_{12}/\text{MPa}$	$T/\text{K}$	$H_{12}/\text{MPa}$
338.15	14.8	313.15	8.8
343.15	15.7	323.15	10.3
348.15	16.6	333.15	11.9
353.15	17.6	343.15	13.6
358.15	18.5	353.15	15.0
363.15	19.2	363.15	16.7

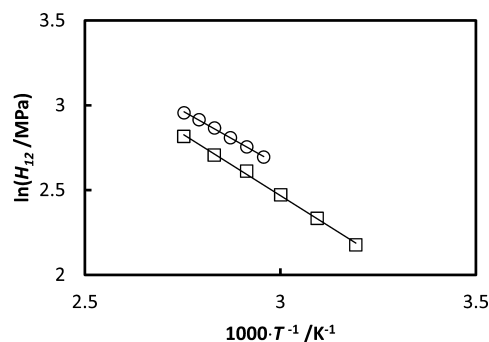


**Figure 7.** Determination of the enthalpy of absorption for  $\text{CO}_2$  in  $[\text{tbma}][\text{MeSO}_4]$  (circles) and  $[\text{tbmp}][\text{MeSO}_4]$  (squares) by plotting the logarithm of the Henry constant against the reciprocal of the temperature.

conditions (i.e., low  $\text{CO}_2$  partial pressures). Essentially, this holds for all ILs based on physical absorption of  $\text{CO}_2$ . Physical ILs, including those measured in this study, could be used at high pressure applications such as the natural gas sweetening process. However, the relatively high melting point and viscosity of the investigated ILs may form a barrier for application even at high pressures. The price/performance ratio of the investigated ILs is simply not sufficient to compete with existing or commercialized physical solvents (e.g., Selexol).



## CONCLUSIONS

The solubility of CO<sub>2</sub> in the ILs tributylmethylammonium methylsulfate [TBMA][MeSO<sub>4</sub>] and tributylmethylphosphonium methylsulfate [TBMP][MeSO<sub>4</sub>] have been determined using a synthetic method. CO<sub>2</sub> solubilities in [TBMA][MeSO<sub>4</sub>] are slightly lower than in [TBMP][MeSO<sub>4</sub>], but the solubility in both ILs is surprisingly higher than in 1-butyl-3-methylimidazolium methylsulfate [bmim][MeSO<sub>4</sub>]. However, the solubilities in the [MeSO<sub>4</sub>] ILs were significantly lower than in the commonly used [bmim][Tf<sub>2</sub>N] IL. These results support the finding that anions dominate the dissolution behavior of CO<sub>2</sub> in ILs, whereas the cations play a minor role.<sup>11</sup> Unfortunately, the low CO<sub>2</sub> solubility of the two measured ILs and the relatively high melting point of these ILs may limit their application at postcombustion capture conditions. Nevertheless, we feel that using the relatively inexpensive and less complex ammonium or phosphonium ILs, after fine-tuning, may help overcoming the cost barrier for applications at large scale.

## AUTHOR INFORMATION

### Corresponding Author

\*E-mail: t.w.delooos@tudelft.nl.

### Funding

Financial support by the Advanced Dutch Energy Materials program of the Dutch Ministry of Economic Affairs, Agriculture, and Innovation.

### Notes

The authors declare no competing financial interest.

## ACKNOWLEDGMENTS

We thank Ir. E. J. M. Straver for his assistance with the experimental work.

## REFERENCES

- (1) Blanchard, L. A.; Hancu, D.; Beckman, E. J.; Brennecke, J. F. Green processing using ionic liquids and CO<sub>2</sub>. *Nature* **1999**, *399*, 28–29.
- (2) Berthod, A.; Ruiz-Angel, M. J.; Carda-Broch, S. Ionic liquids in separation techniques. *J. Chromatogr., A* **2008**, *1184*, 6–18.
- (3) Freemantle, M. *An Introduction to Ionic Liquids*; RSC Publishing: London, U.K., 2010.
- (4) Parvulescu, V. I.; Hardacre, C. Catalysis in ionic liquids. *Chem. Rev.* **2007**, *107*, 2615–2665.
- (5) Buzzeo, M. C.; Evans, R. G.; Compton, R. G. Non-Haloalumininate room-temperature ionic liquids in electrochemistry: a review. *ChemPhysChem* **2004**, *5*, 1106–1120.
- (6) Blanchard, L. A.; Brennecke, J. F. Recovery of organic products from ionic liquids using supercritical carbon dioxide. *Ind. Eng. Chem. Res.* **2001**, *40*, 287–292.
- (7) D'Alessandro, D. M.; Smit, B.; Long, J. R. Carbon dioxide capture: prospects for new materials. *Angew. Chem., Int. Ed.* **2010**, *49*, 6058–6082.
- (8) Brennecke, J. F.; Gurkan, B. E. Ionic liquids for CO<sub>2</sub> capture and emission reduction. *J. Phys. Chem. Lett.* **2010**, *1*, 3459–3464.
- (9) Aki, S. N. V. K.; Mellein, B. R.; Saurer, E. M.; Brennecke, J. F. High-pressure phase behavior of carbon dioxide with imidazolium-based ionic liquids. *J. Phys. Chem. B* **2004**, *108*, 20355–20365.
- (10) Muldoon, M. J.; Aki, S. N. V. K.; Anderson, J. L.; Dixon, J. K.; Brennecke, J. F. Improving carbon dioxide solubility in ionic liquids. *J. Phys. Chem. B* **2007**, *111*, 9001–9009.
- (11) Anthony, J. L.; Anderson, J. L.; Maginn, E. J.; Brennecke, J. F. Anion effects on gas solubility in ionic liquids. *J. Phys. Chem. B* **2005**, *109*, 6366–6374.
- (12) Cadena, C.; Anthony, J. L.; Shah, J. K.; Morrow, T. I.; Brennecke, J. F.; Maginn, E. J. Why is CO<sub>2</sub> so soluble in imidazolium-based ionic liquids? *J. Am. Chem. Soc.* **2004**, *126*, 5300–5308.
- (13) Maginn, E. J. Molecular simulation of ionic liquids: current status and future opportunities. *J. Phys.: Condens. Matter* **2009**, *21*, 1–17.
- (14) Maginn, E. J. Atomistic simulation of the thermodynamic and transport properties of ionic liquids. *Acc. Chem. Res.* **2007**, *40*, 1200–1207.
- (15) Huang, J.; Rüther, T. Why are ionic liquids attractive for CO<sub>2</sub> absorption? An overview. *Aust. J. Chem.* **2009**, *62*, 298–308.
- (16) Mattedi, S.; Carvalho, P. J.; Coutinho, J. A. P.; Alvarez, V. H.; Iglesias, M. High pressure CO<sub>2</sub> solubility in N-methyl-2-hydroxyethylammonium protic ionic liquids. *J. Supercrit. Fluids* **2011**, *56*, 224–230.
- (17) Yuan, X.; Zhang, S.; Liu, J.; Lu, X. Solubilities of CO<sub>2</sub> in hydroxyl ammonium ionic liquids at elevated pressures. *Fluid Phase Equilib.* **2007**, *257*, 195–200.
- (18) Condemarin, R.; Scovazzo, P. Gas permeabilities, solubilities, diffusivities, and diffusivity correlations for ammonium-based room temperature ionic liquids with comparison to imidazolium and phosphonium RTIL data. *Chem. Eng. J.* **2009**, *147*, 51–57.
- (19) Carvalho, P. J.; Alvarez, V. H.; Marrucho, I. M.; Aznar, M.; Coutinho, J. A. P. High carbon dioxide solubilities in trihexyltetradecylphosphonium-based ionic liquids. *J. Supercrit. Fluids* **2010**, *52*, 258–265.
- (20) Gurkan, B. E.; de la Fuente, J.; Mindrup, E. M.; Ficke, L. E.; Goodrich, B. F.; Price, E. A.; Schneider, W. F.; Brennecke, J. F. Equimolar CO<sub>2</sub> absorption by anion-functionalized ionic liquids. *J. Am. Chem. Soc.* **2010**, *132*, 2116–2117.
- (21) Anderson, J. L.; Dixon, J. K.; Brennecke, J. F. Solubility of CO<sub>2</sub>, CH<sub>2</sub>, C<sub>2</sub>H<sub>6</sub>, C<sub>2</sub>H<sub>4</sub>, O<sub>2</sub> and N<sub>2</sub> in 1-hexyl-3-methylpyridinium bis(trifluoromethylsulfonyl)imide: comparison to other ionic liquids. *Acc. Chem. Res.* **2007**, *40*, 1208–1216.
- (22) Galán Sánchez, L. M. Ph.D. thesis, Eindhoven University of Technology, 2008.
- (23) Kumelan, J.; Tuma, D.; Perez-Salado Kamps, A.; Maurer, G. Solubility of the single gases carbon dioxide and hydrogen in the ionic liquid [bmpp][Tf<sub>2</sub>N]. *J. Chem. Eng. Data* **2010**, *55*, 165–172.
- (24) Song, H. N.; Lee, B.; Lim, J. S. Measurement of CO<sub>2</sub> solubility in ionic liquids: [BMP][TfO] and [P14,6,6,6][Tf<sub>2</sub>N] by measuring bubble-point pressure. *J. Chem. Eng. Data* **2010**, *55*, 891–896.
- (25) Yim, J.; Song, H. N.; Yoo, K.; Lim, J. S. Measurement of CO<sub>2</sub> solubility in ionic liquids: [BMP][Tf<sub>2</sub>N] and [BMP][MeSO<sub>4</sub>] by measuring bubble-point pressure. *J. Chem. Eng. Data* **2011**, *56*, 1197–1203.
- (26) Accelerating Ionic Liquid Commercialization. [http://www.chemicalvision2020.org/pdfs/ionicliquid\\_commercialization.pdf](http://www.chemicalvision2020.org/pdfs/ionicliquid_commercialization.pdf) (accessed Feb 20, 2012).
- (27) Joglekar, H. G.; Rahman, I.; Kulkarni, B. D. The path ahead for ionic liquids. *Chem. Eng. Technol.* **2007**, *30*, 819–828.
- (28) de Loos, T. W.; van der Kooi, H. J.; Ott, P. L. Vapor-liquid critical curve of the system ethane + 2-methylpropane. *J. Chem. Eng. Data* **1986**, *31*, 166–168.
- (29) Shariati, A.; Peters, C. J. High-pressure phase behavior of systems with ionic liquids: II. The binary system carbon dioxide + 1-ethyl-3-methylimidazolium hexafluorophosphate. *J. Supercrit. Fluids* **2004**, *29*, 43–48.
- (30) Shariati, A.; Peters, C. J. High-pressure phase behavior of systems with ionic liquids: III. The binary system carbon dioxide + 1-hexyl-3-methylimidazolium hexafluorophosphate. *J. Supercrit. Fluids* **2004**, *30*, 139–144.
- (31) Kumelan, J.; Perez-Salado Kamps, A.; Tuma, D.; Maurer, G. Solubility of CO<sub>2</sub> in the ionic liquids [bmim][CH<sub>3</sub>SO<sub>4</sub>] and [bmim][PF<sub>6</sub>]. *J. Chem. Eng. Data* **2006**, *51*, 1802–1807.
- (32) Raeissi, S.; Peters, C. J. Carbon dioxide solubility in the homologous 1-alkyl-3-methylimidazolium bis-(trifluoromethylsulfonyl)imide family. *J. Chem. Eng. Data* **2009**, *54*, 382–386.

(33) Span, R.; Wagner, W. A new equation of state for carbon dioxide covering the fluid region from the triple-point temperature to 1100 K at pressures up to 800 MPa. *J. Phys. Chem. Ref. Data* **1996**, 25, 1509–1596.